ISCI, Volume *20*

Supplemental Information

CIDEA Transcriptionally Regulates UCP1 for Britening and Thermogenesis in Human Fat Cells

Sukanta Jash, Sayani Banerjee, Mi-Jeong Lee, Stephen R. Farmer, and Vishwajeet Puri

SUPPLEMENTAL DATA

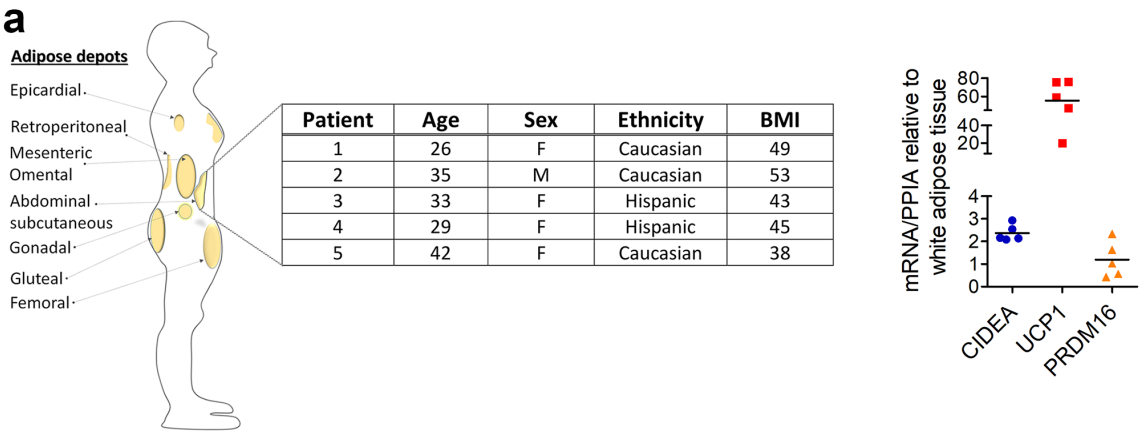

Patient	Age	Sex	Ethnicity	BMI
1	26	F	Caucasian	49
2	35	M	Caucasian	53
3	33	F	Hispanic	43
4	29	F	Hispanic	45
5	42	F	Caucasian	38

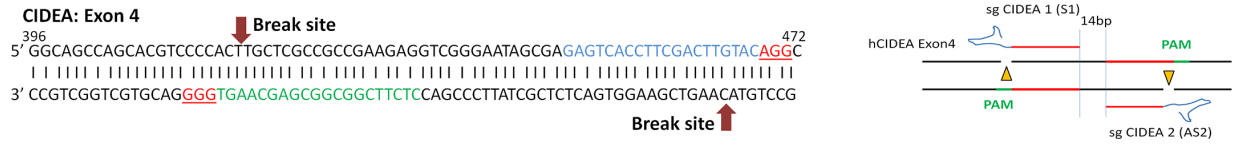

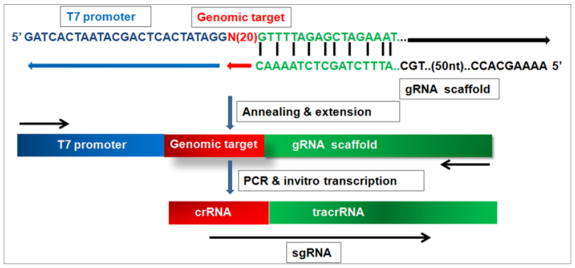

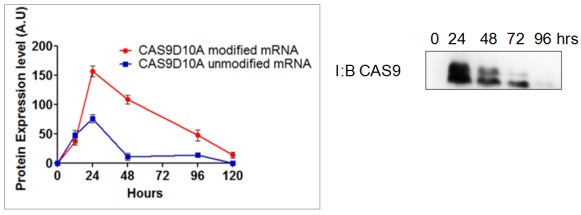

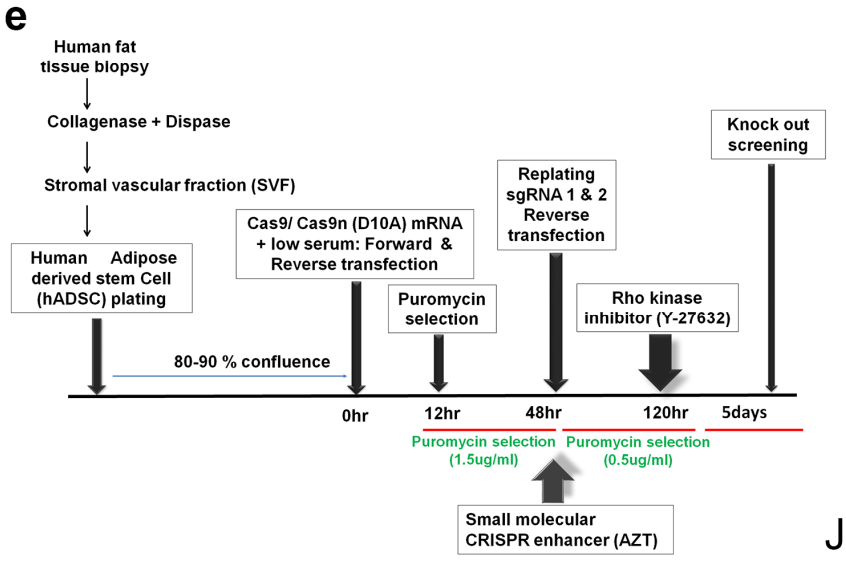

Jash et al., Figure S1

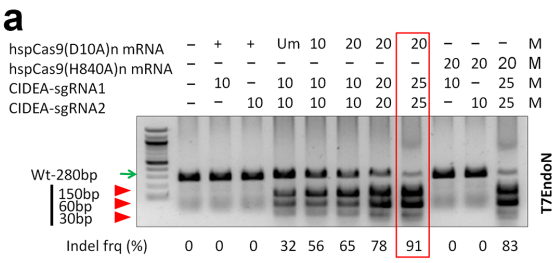

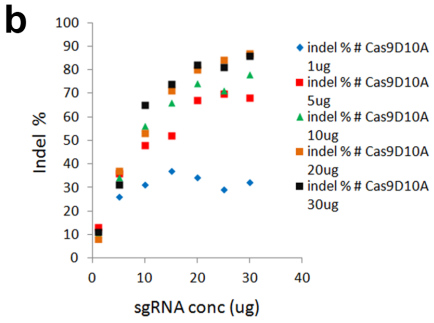

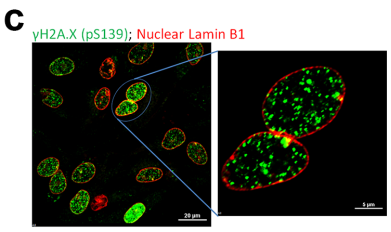

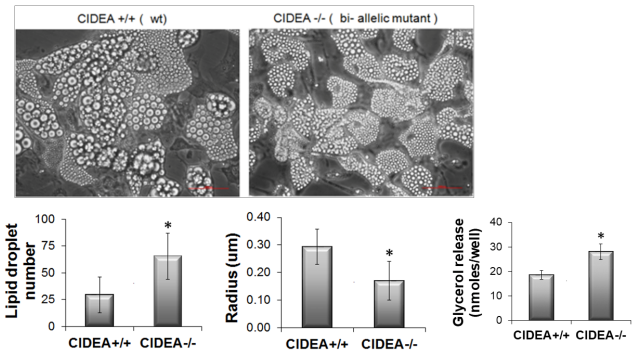

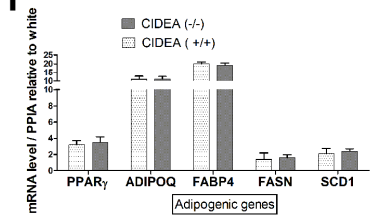

g

	Sense(S)	Sequence (5'-3')	Mismatches	Chr	Gene
On target	S1	GAGTCACCTTCGACTTGTACAGG	0	Chr18	CIDEA
Off target	S2	GATTCACCTTTGACGTGTACAAG	3	Chr 14	CIDEB
	S3	GTGTAACCTTTGACCTGTACAAG	4	Chr 3	CIDECP
	S4	TAGTCTCCTTCAACTTGTATTGG	4	Chr 2	APOB
	S5	GTGTCACCTACTACTTGGACTGG	4	Chr 16	TPSB2
	S6	GTGTCACCTACTACTTGGACTGG	4	Chr 16	TPSB1
	S7	GTGTCACCTACTACTTGGACTGG	4	Chr 16	TPSD1
	S8	GAGTGACGTTTGACTGGTACAGG	4	Chr 6	VIP
	S9	GAGTCAGCTTGAACTTGTAGTAG	4	Chr 9	ZER1

	Antisense(AS)	Sequence (5'-3')	Mismatches	Chr	Gene
On target	AS2	CTCTTCGGCGGCGAGCAAGTGGG	0	Chr18	CIDEA
Off target	AS10	CTCTTCTTCTGCAAGCAAGTGGG	4	Chr 1	PABPC4
	AS11	CTCTTCGGCGGTGCGCAAGGCGG	3	Chr 9	FBP1
	AS12	CCCTTCGGCGCCGACCAGGTGAG	4	Chr 12	SLC15A4
	AS13	CTCTTCGGCAGCATGCAGGTGAG	4	Chr 1	RNF207
	AS14	CTCTTTGGCGGCGGCCCAGTCGG	4	Chr 16	PHKG2

Jash et al., Figure.S2

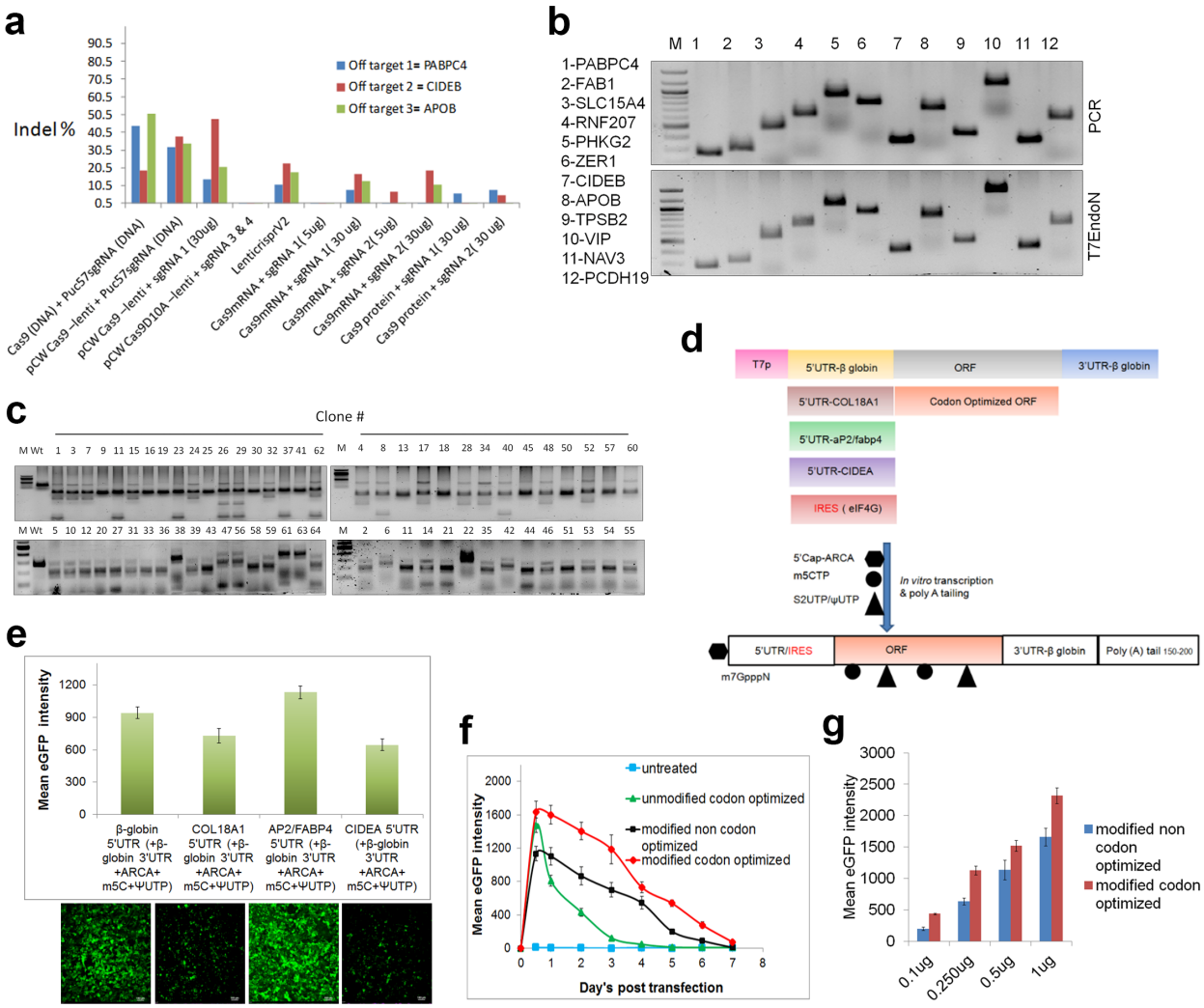

Jash et al., Figure S3

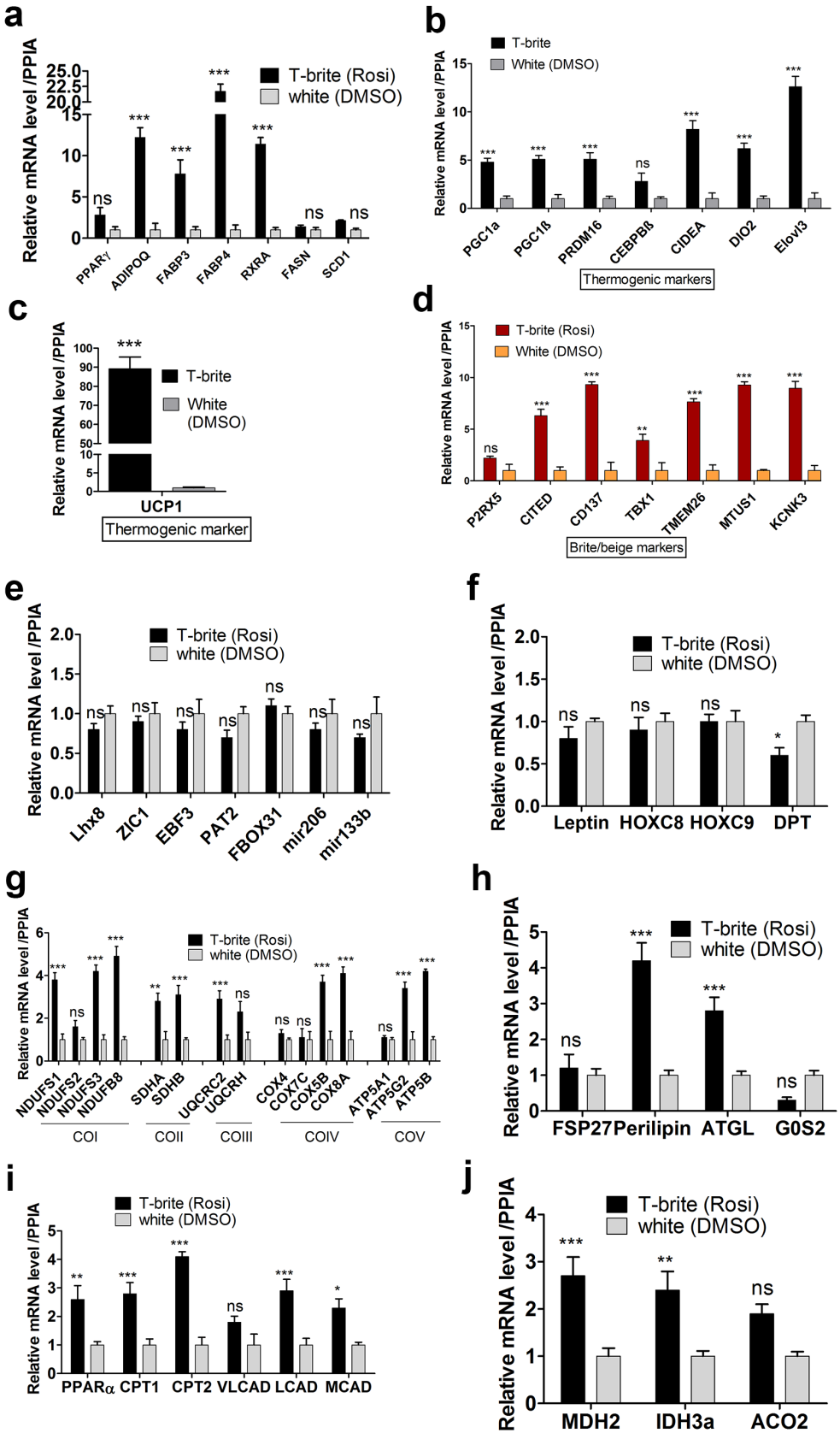

Jash et al., Figure S4

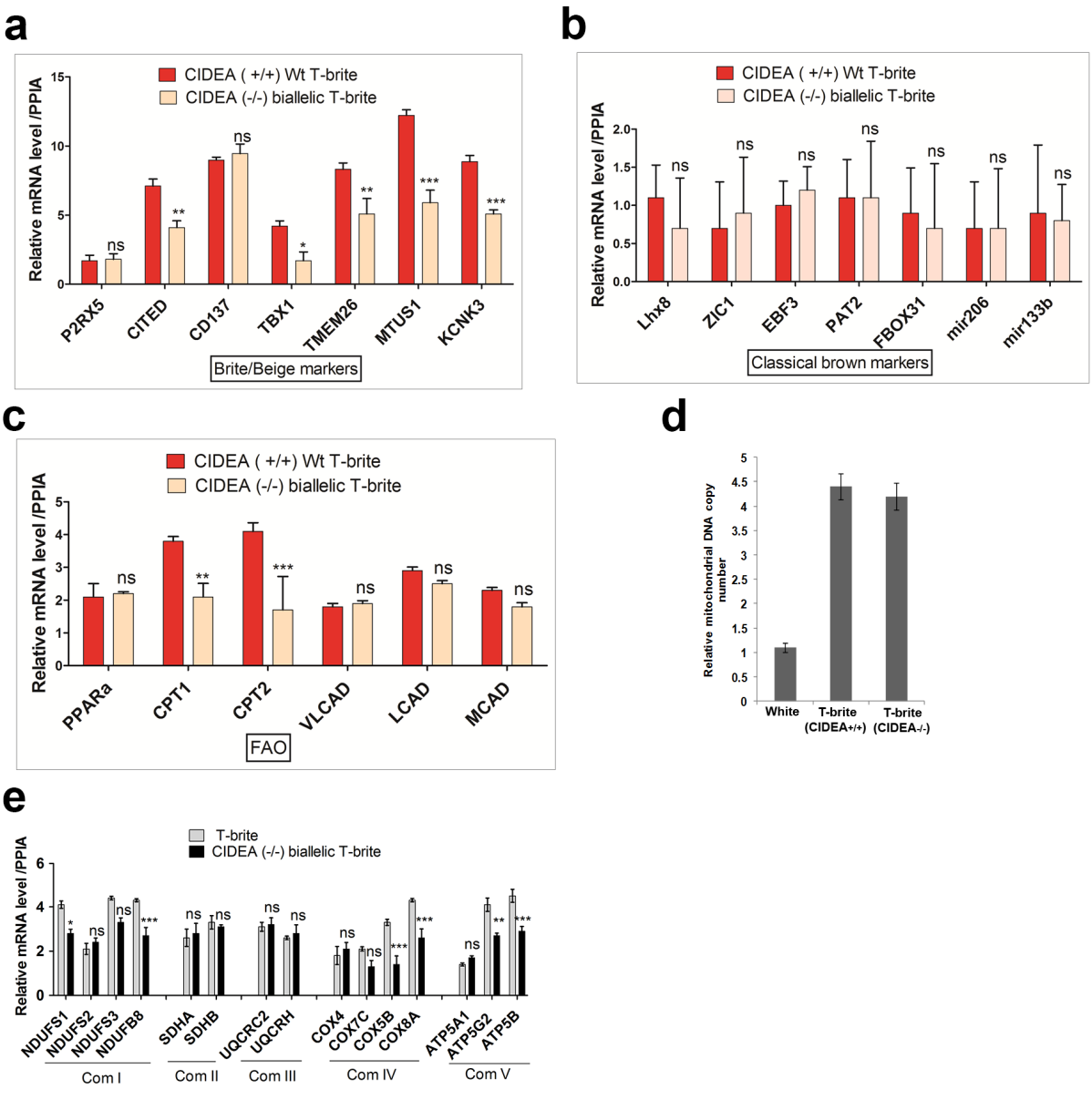

Jash et al., Figure S5

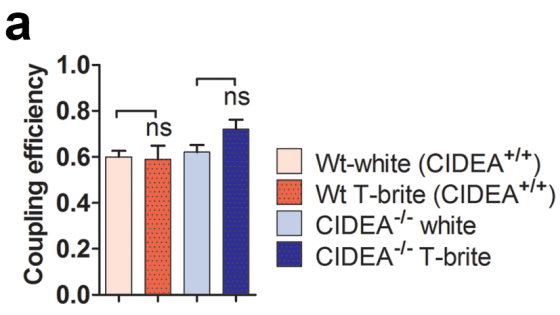

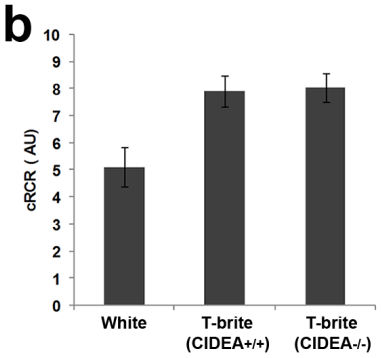

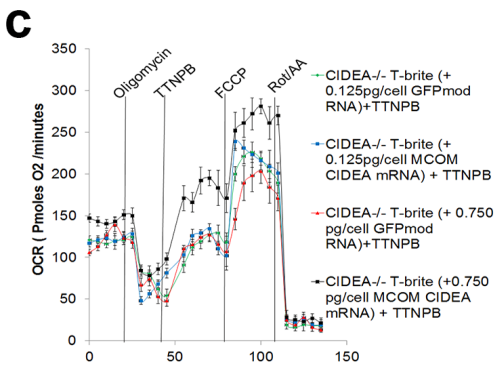

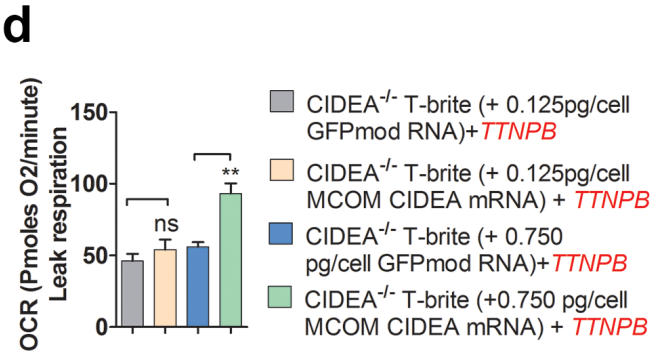

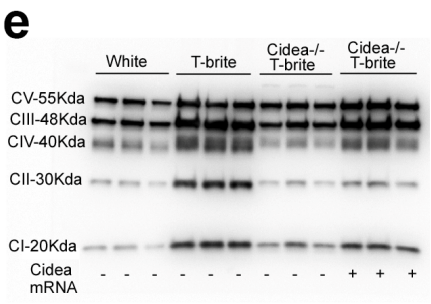

Jash et al., Figure S6

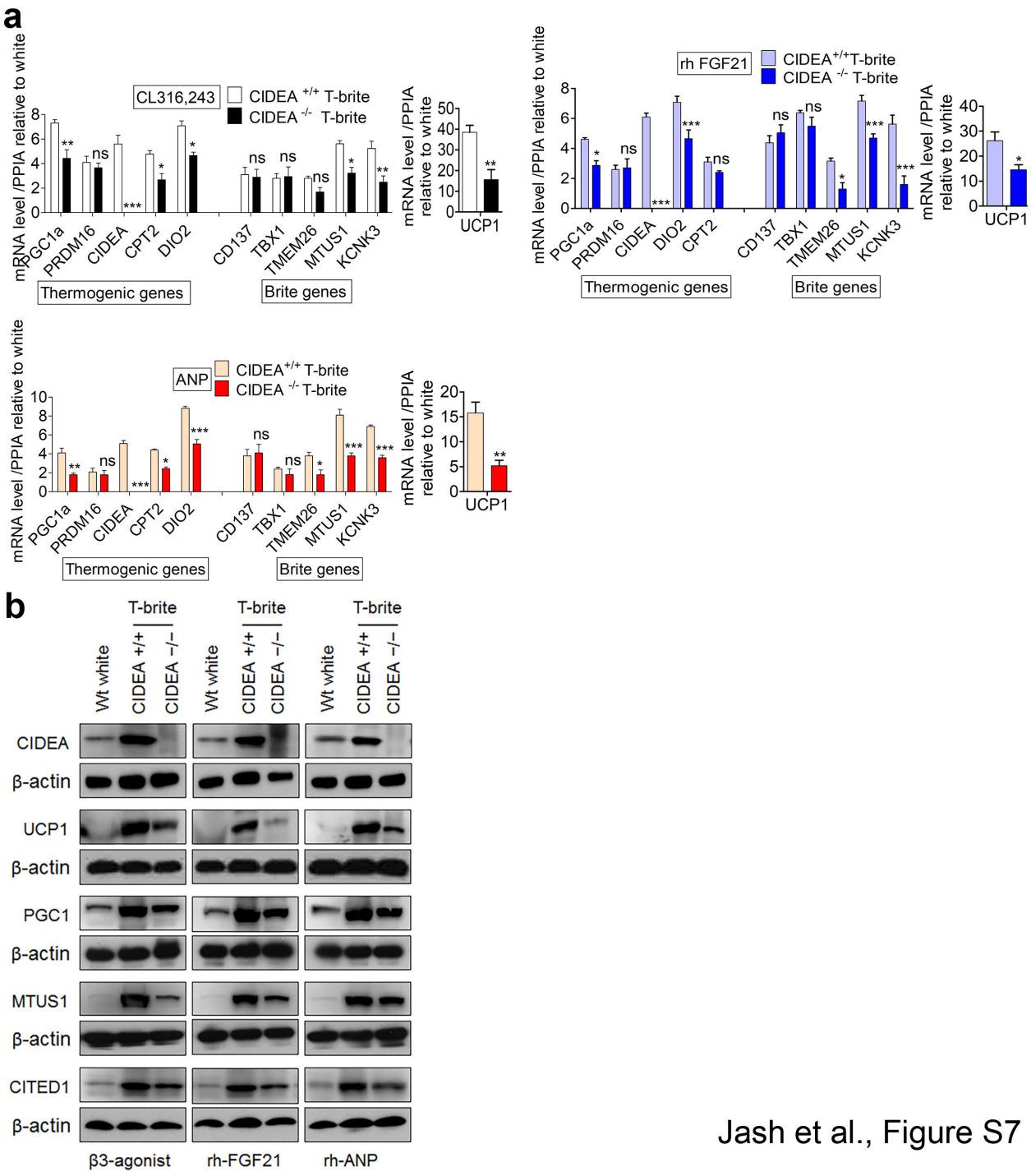

Jash et al., Figure S7

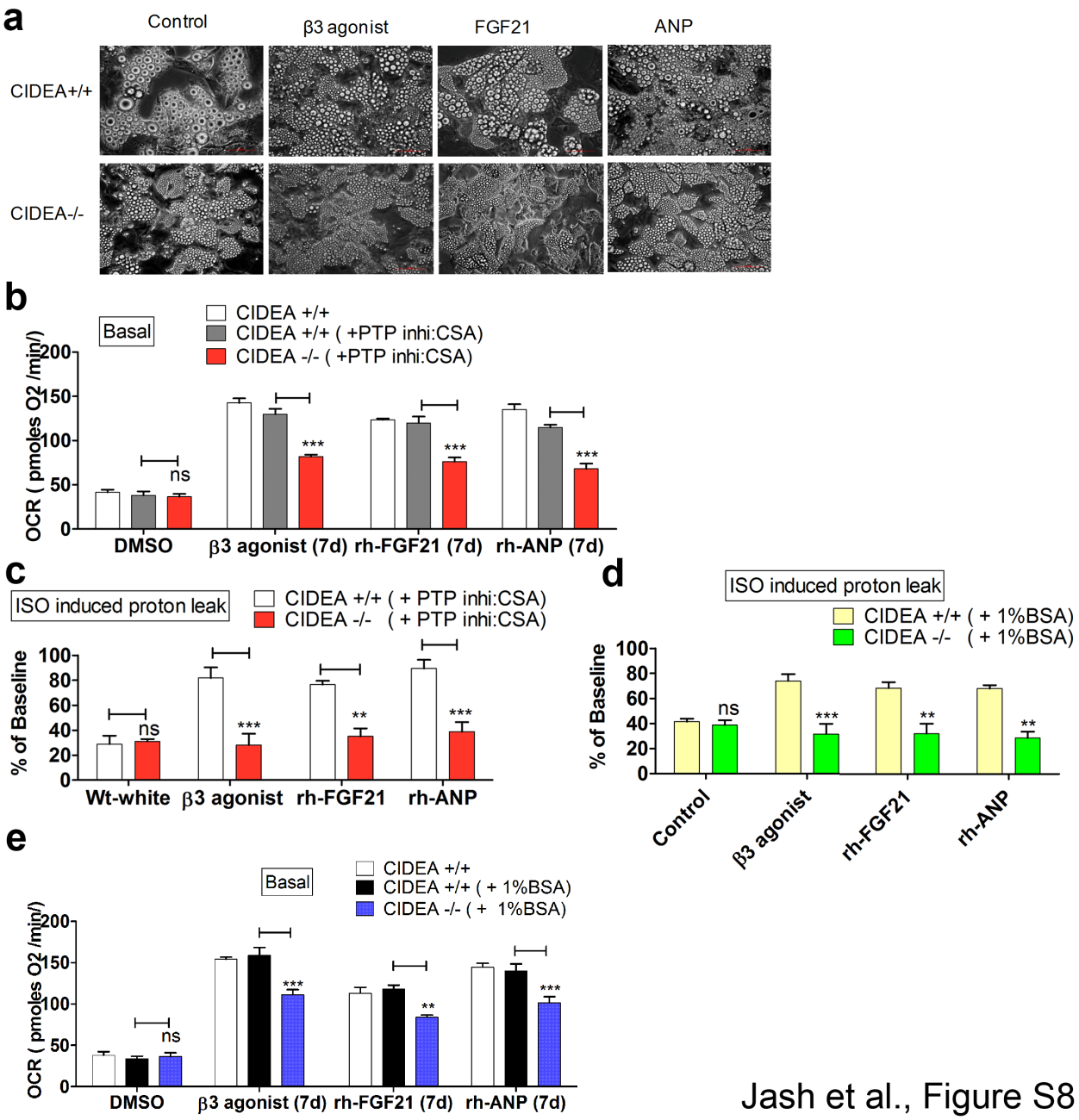

Jash et al., Figure S8

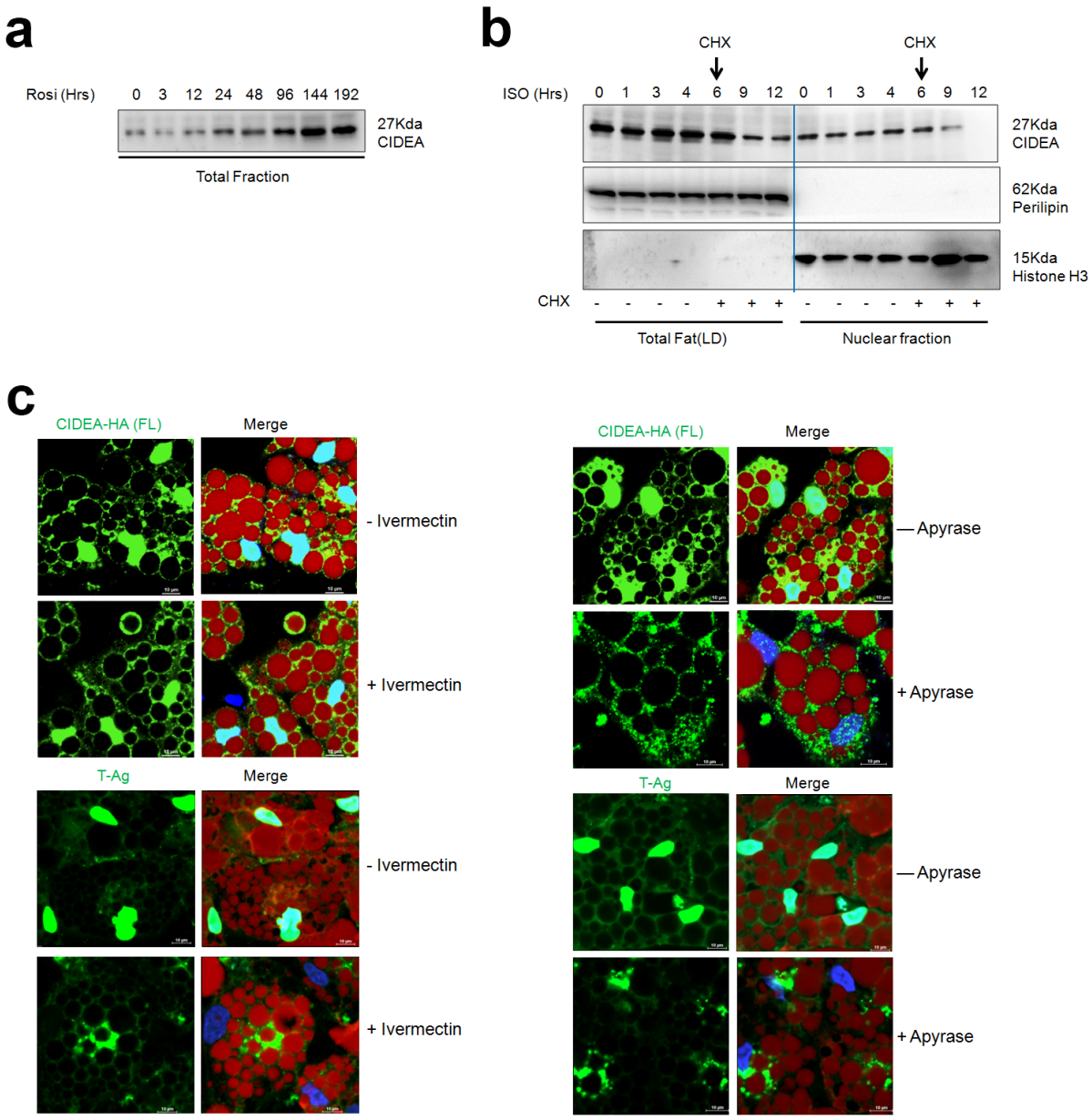

Jash et al., Figure S9

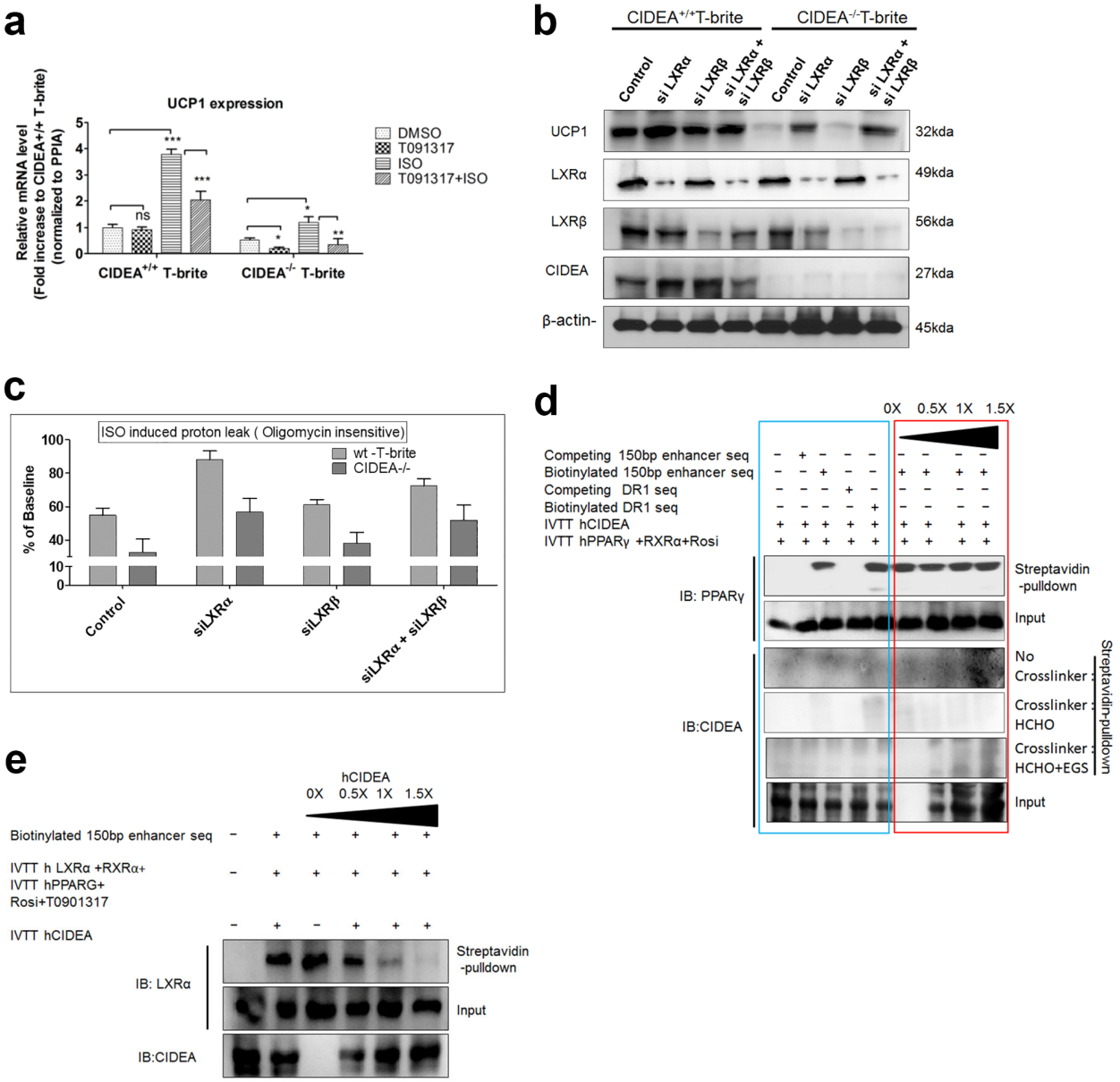

Jash et al., Figure S10

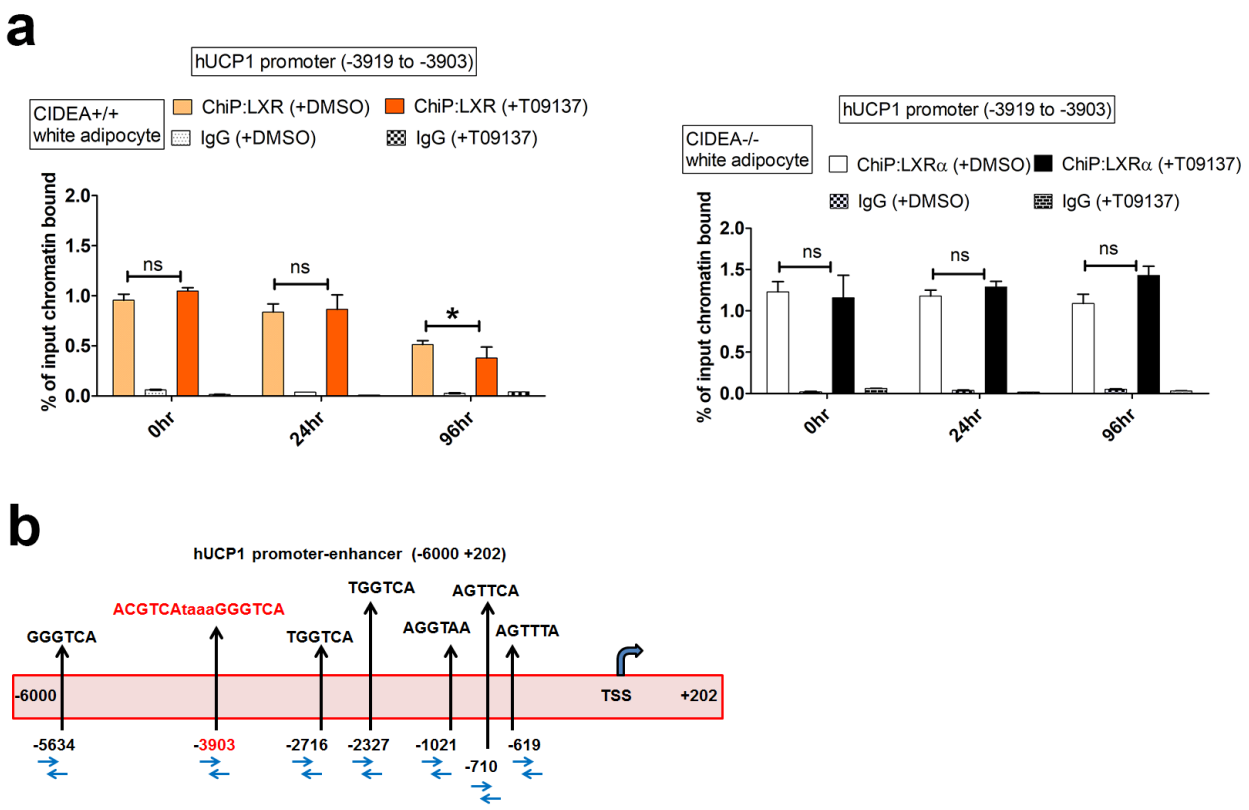

Jash et al, Figure S11

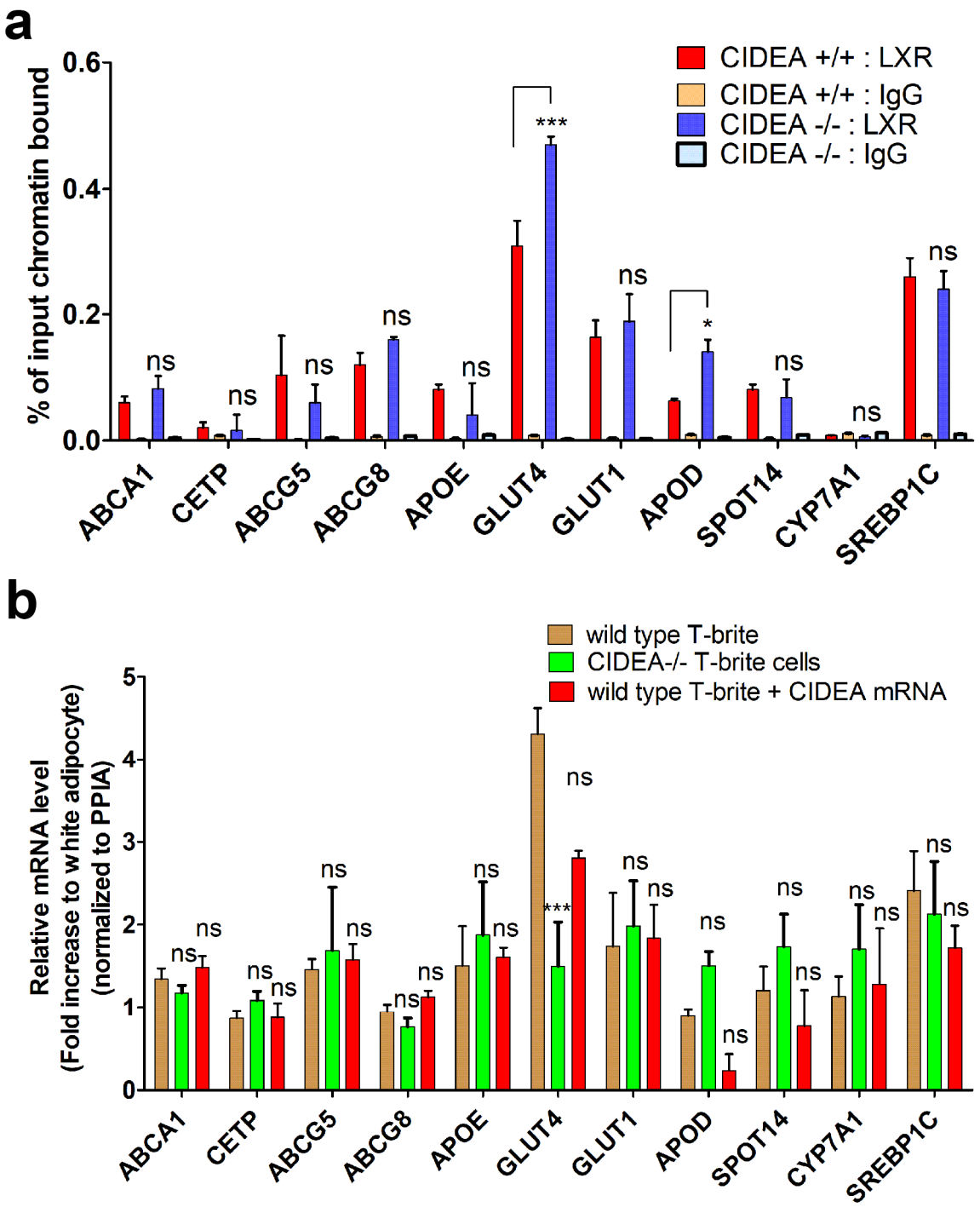

Jash et al., Figure S12

SUPPLEMENTARY FIGURE LEGENDS

Figure S1, Related to Figure 1. Construction and synthesis of CRISPR-Cas9 for targeting hCIDEA. (**a**) Origin of subcutaneous adipose explants from five obese human subjects (left); induction of CIDEA and UCP1 with 1 μM Rosi for 7 d (right). (**b**) Top: hCIDEA exon 4 targeted by S (sgRNA2) and AS (sgRNA1) sgRNA for double nicking; target sites are highlighted in green (sgRNA1) and blue (sgRNA2), and PAMs are underlined (red). Bottom: sgRNA binding and 14-bp offset between S and AS sgRNAs for efficient targeting and double nicking. (**c**) Hybridization of the T7 promoter-containing sgRNA oligo template and sgRNA scaffold template followed by template purification and *in vitro* transcription of the sgRNA template with modified nts. (**d**) Left: Time course of modified and unmodified Cas9D10A expression in human preadipocytes after Cas9D10A transfection. Data are mean ± SEM (n = 3). Right: Western blot showing Cas9 expression. (**e**) Schematic workflow of CRISPR-Cas9D10A nickase-mediated CIDEA KO generation in primary human preadipocytes.

Figure S2, Related to Figure 1. Developing CRISPR-Cas9nD10A for CIDEA KO. (**a**) Titration of mod S and AS sgRNAs targeting hCIDEA- and Cas9D10A-mod mRNA for double nickase analysis. Y-axis shows insertion/deletion (indel) frequencies. Five off-target sites homologous for each CIDEA sgRNA were chosen based on mismatched nt positions. (**b**) Titration of S and AS sgRNAs targeting hCIDEA and Cas9D10A mod mRNA for evaluation of double nicking efficiency. Indel frequencies were determined with T7EndoN assays (each datum represents 3 separate experiments). (**c**) Double stranded break-specific nuclear localization of phosphorylated γH2A.X in hADSCs showing efficiency of dual RNA-mediated CRISPR-Cas9

nickase. (**d**) mutation patterns detected by PCR amplification and Sanger sequencing. Wt, clones without indels. BA-Het, clones with biallelic heterogenous indel mutations in both alleles. BA-Homo, clones with biallelic homogenous indel mutations in both alleles (sgRNA1 and sgRNA2 target sites are in blue and green, respectively; PAM sites are underlined red). Dotted line, deletions; lower case orange letters, inserted sequences. Deleted (Δ) and inserted (+) nucleotides identified by Sanger sequencing are indicated to the right of each allele. (**e**) Representative phase-contrast images showing smaller LDs in CIDEA$^{-/-}$ white adipocytes than in WT [CIDEA$^{+/+}$(wt)] white adipocytes. Lower panels show morphometric analysis of the number and radius of lipid droplets, and biochemical quantification of basal lipolysis based on measurement of glycerol release after 2 hours. Results for lipid droplet number and radius are an average of at least 10 cells from the same cover slip and/or the same field in three independent experiments. Data are mean ± SEM (n = 3). (**f**) mRNA levels of adipogenic markers in CIDEA$^{+/+}$ and CIDEA$^{-/-}$ adipocytes. Data are mean ± SEM (n = 3). (**g**) S (n = 8) and AS (n = 6) sgRNA target sites assessed according to software prediction. Mismatch nts are indicated in red and PAM motifs are underlined.

Figure S3, Related to Figure 1. Developing CRISPR-Cas9nD10A for CIDEA KO, and mod mRNA for CIDEA expression in human adipocytes. (**a**) Off-target cleavage by Cas9 and Cas9D10A with A or AS sgRNAs alone or in combination. Note that there were no off-target effects with Cas9D10A. (**b**) Representative T7EndoN analysis of high-scoring off-targets. (**c**) T7EndoN analysis of human preadipocyte clones after CRISPR-Cas9 nickase-mediated CIDEA KO. (**d**) CIDEA constructs for generation of CIDEA mod mRNA by *in vitro* transcription. Note the different 5'UTRs used with the beta-globin 3'UTR. CIDEA ORF was optimized for human

codon usage. The identities and quantities of modified and unmodified nucleotides used are presented in the methods section. (**e**) Confocal microscopic expression analysis of mod GFP mRNA construct with different 5'UTRs after single transfection into mature adipocytes. The AP2/FABP4 5'UTR was used in our further analysis. We observed 85–90% transfection with mod green fluorescent protein (GFP) mRNA in mature adipocytes; GFP expression varied across 5'UTR types, with AP2 5'UTR yielding particularly strong ribosome binding and translatability. Data are mean ± SEM (n = 3). (**f**) Confocal microscopic time-course expression analysis of GFP mRNA with or without modified nts and codon optimization after single transfection into mature human adipocytes. The expression and stability of mod GFP mRNA were improved by nt mod and codon optimization. In mature adipocytes, mod GFP was expressed within 3 h, peaked after 12–24 h, and declined to basal levels by 6–7 d. Data are mean ± SEM (n = 3). (**g**) Dose-dependent GFP expression in mature adipocytes with and without codon optimization. Data are mean ± SEM (n = 3).

Figure S4, Related to Figure 1. Rosi-induced britening of human white adipocytes.

hADSCs derived from subcutaneous abdominal adipose were differentiated and then treated with 1 μM Rosi for 7 d. The y-axis shows the relative mRNA levels of (**a**) differentiation markers common to white and brite/beige, (**b**) brite/beige fat cell-selective genes, (**c**) UCP1 expression, (**d**) brite markers, (**e**) white adipose-selective genes, (**f**) brown markers, (**g**) mitochondrial oxidative phosphorylation genes, (**h**) major lypolytic genes, and (**i**) FAO, and (**j**) TCA genes. Each datum represents a mean fold change ± SEM (vs. DMSO-treated controls) of pooled fractions from three donors. ***P < .001, **P < .01, and *P < .05, two-way ANOVA followed by Bonferroni post-test.

Figure S5, Related to Figure 1. CIDEA KO inhibits britening and uncoupling in human adipocytes. Real-time qPCR analysis of the differential expression of (**a**) brite markers, (**b**) brown markers, and (**c**) FAO-related genes in CIDEA$^{+/+}$ (identified as Wt) versus biallelic CIDEA$^{-/-}$ T-brites. Mean fold changes ± SEM (vs. DMSO-treated controls) of five independent experiments are shown. (**d**) Relative mitochondrial DNA copy number in T-brites was unaffected by KO of CIDEA (T-brite CIDEA$^{-/-}$). Data are mean ± SEM (n = 3). (**e**) Expression of oxidative phosphorylation genes in WT CIDEA$^{+/+}$ versus CIDEA$^{-/-}$ T-brites. ***P < .001, **P < .01, and *P < .05, two-way (a–c) or one-way (e) ANOVA followed by Bonferroni multi-comparison tests.

Figure S6, Related to Figure 2. CIDEA KO inhibits OCR in human white adipocytes. (**a**) Quantification of coupling efficiency of the samples in Fig. 2e. Data are mean ± SEM (n = 3). (**b**) Cell respiratory control ratio (cRCR) in white adipocytes, CIDEA+/+ and CIDEA-/- T-brites. Data are mean ± SEM (n = 3). (**c**) OCR increases following TTNPB (50 μm) treatment of CIDEA$^{-/-}$ T-brites transfected with control-GFP mRNA or mcom-CIDEA mRNA. (**d**) TTNPB-induced increase in CIDEA$^{-/-}$ T-brite leak respiration correlated with the amount of mcom CIDEA mRNA delivered. Data are mean ± SEM (n = 3). **P < .01, two-way ANOVA followed by Bonferroni multi-comparison tests. (**e**) Relative levels of oxidative phosphorylation subunits (CV-α [Atp5B], CIII-core2 [UQCRC2], CII-30 [SDHB], CIV-II [CytC-OxII], CI-20 [NdufB8]) in WT and KO T-brites. After a 7-d Rosi treatment, CIDEA$^{-/-}$ adipocytes were transfected with 0.750 pg/cell mcom-CIDEA mRNA or GFP control mRNA for 3 d (last three lanes). For Seahorse experiments 24 well plates seeded with equal number of cells were used. After

completion of the oxygen consumption measurement, each well in every experiment was found to have 10-12 μg total protein.

Figure S7, Related to Figure 2. CIDEA is critical for human white adipocyte britening by various activators/inducers. (**a**) Quantitative reverse transcriptase (qRT)-PCR analysis of thermogenic and britening markers following induction of human white adipocytes with β3-agonist (CL 316,243), FGF21, and ANP in the presence or absence of CIDEA. UCP1 expression was reduced in CIDEA-/- T-brites. Data are expressed as mean (±SEM) of five independent experiments; ***P < .001, **P < .01, and *P < .05, two-way ANOVA followed by Bonferroni multi-comparison tests. (**b**) CIDEA, UCP1, PGC1α, MTUS1, and CITED1 protein expression in T-brites following induction with various inducers in the presence or absence of CIDEA.

Figure S8, Related to Figure 2. Britening of human adipocytes by different britening-inducers is CIDEA dependent.

(a) Representative phase-contrast images of adipocytes britened by each of several activators/inducers in WT CIDEA+/+ versus KO CIDEA-/- (KO conducted in preadipocytes before differentiation). (**b**) Basal respiration (OCR in pmoles O_2/min), and (**c**) ISO-induced proton leak respiration (OCR as % baseline) of T-brites generated by different stimuli. Before OCR measurements, cells were pretreated with the PTP inhibitor CSA. (**d**) Iso-induced proton leak, and **(e)** basl OCR was reduced in $CIDEA^{-/-}$ versus $CIDEA^{+/+}$ T-brites; 1% BSA was added to quench excess FFA activity. In b,c,d and e, the results are mean ± SEM of three independent experiments. ***P < .001 and **P < .01, one-way ANOVA followed by Bonferroni multi-comparison tests.

Figure S9, Related to Figure 4. Lipid droplet to nuclear shuttling of CIDEA.

(**a**) Time courses of CIDEA protein expression in human white adipocytes after addition of 1 μm Rosi. (**b**) Effect of cycloheximide (CHX) on the ISO-induced subcellular distribution and nuclear enrichment of CIDEA. (**c**) Confocal images of T-brites expressing CIDEA-HA or SV-40 T-Ag GFP-NLS showing that, after 24-h transfection, 6-h 50 μM ivermectin treatment did not prevent CIDEA import, but blocked α/β importin reognition of HA-t-Ag incorporated NLS, whereas 6-h apyrase (0.1 U/ml) reduced nuclear import of CIDEA.

Figure S10, Related to Figure 5. CIDEA regulates UCP1 expression via LXRα.

(**a**) The LXR ligand T091317, which did not alter mean (±SEM) UCP1 expression in WT T-brites not treated with ISO, reduced *UCP1* mRNA expression in CIDEA$^{-/-}$ T-brites and in ISO-treated WT and KO T-brites. ***P < .001, **P < .01, and *P < .05, two-way ANOVA followed by Bonferroni post-test. (**b**) Loss of UCP1 protein in CIDEA$^{-/-}$ T-brites was reversed by introduction of LXRα suppressing siRNA (with or without LXRβ siRNA). During individual knockdown, 50 nM siRNA concentration was used, whereas, during dual-knockdown 25 nM concentration of each siRNA species was used. Cellular lysates were pooled from T-brites generated from three donors. (**c**) effect of siRNA-mdeiated LXRα and/or LXRβ depletion on iso-induced proton leak in T-brite adipocytes ±CIDEA. Data are mean ± SEM (n = 3). (**d**) Protein-DNA binding analysis of recombinant hCIDEA with dUER$_{150bp}$ DNA, including DR4, in the presence of recombinant human PPARγ (hPPARγ) and its heterodimeric partner RXRα (blue box). The hPPARγ-dUER$_{150bp}$ interaction strength was unaffected by CIDEA levels (red box). No CIDEA was recovered by streptavidin pull-down followed by western blotting, with or

without a crosslinker. (**e**) Analysis of LXRα and PPARγ proteins with $dUER_{150bp}$ DNA, which includes DR4 and DR1, in the presence of equimolar amounts of hCIDEA, hPPARγ and RXRα.

Figure S11, Related to Figure 6. CIDEA interacts with LXR to regulate UCP1 transcription. (**a**) ChIP-qPCR analysis of LXRα binding to UCP1 promoter-enhancer at -3919 during Rosi-induced britening of $CIDEA^{+/+}$ (left) or $CIDEA^{-/-}$ (right) adipocytes in the presence of LXR ligand T09137. Data are mean ± SEM (n = 3). (**b**) Schematic representation of the multiple LXR response elements in the human UCP1 promoter (-6000 to +201). Among seven possible response elements, only the one at -3903 mediates LXRα binding. The half site of each response element is indicated above and the positions of the ChIP primer pairs are indicated below. (**c**) Time-course ChIP-qPCR analysis of LXRα occupancy over six LXR response elements (site loci indicated within parentheses; site at -3909 not included) in the human *UCP1* enhancer during Rosi-mediated britening Data are mean ± SEM (n = 3).

Figure S12, Related to Figure 6. ChIP analysis of LXR regulated genes in the presence and absence of CIDEA. (a) Effect of CIDEA on LXR-regulated genes in T-brite adipocytes. **(b)** Real-time PCR analysis of LXR regulated genes in T-brite adipocytes ± CIDEA. In both a and b, Data are mean ± SEM (n = 3). ***P < 0.001 and *P < .05, two-way ANOVA followed by Bonferroni post-tests.

Data S1, Related to Figures 1-6. mRNA template sequences.

Data S2, Related to Figures 1-6 and S1-S12. Genes, Primer ID and sequences. List of all the genes, their primer IDs, primer sequences used in the study.

TRANSPARENT METHODS

Human subjects. Adipose tissues were obtained from five human patients (mean age 48.6years and BMI 34.6 kg/m^2) during panniculectomy following weight loss. All subjects provided informed consent for participation. The protocol was approved by Institutional Review Board of Boston University Medical Center.

Isolation of hADSCs. Human adipose tissue stromal vascular cells were obtained from Boston Nutrition Obesity Research Center (BNORC). Briefly, abdominal subcutaneous adipose tissue were obtained during elective surgeries from human subjects [BMI, 40.5 ± 1.6 kg/m2 (range 23-63); 41.4 ± 2.0 years (range 25-71) old; 33F, 6M; 11AA, 12H, 17C] who were free of diabetes, cancers, endocrine or inflammatory diseases by medical history. Surgeries took place at the Boston Medical Center. All subjects provided informed consents as approved by Institutional Review Boards of the Boston Medical Center. Adipose tissues were placed in type 1 collagenase (1 mg/ml in Hanks' balanced salt solution) for 2 h (22), and then the hADSCs within them were isolated by filtering with a 250-μm mesh and centrifugation twice at 500 ×*g* for 10 min. Between the centrifugation rounds, cell pellets were treated with erythrocyte lysis buffer [0.154 mM NH_4Cl, 10 mM K_2HPO_4, and 0.1 mM ethylenediaminetetraacetic acid (EDTA), pH 7.3]. The re-pelleted cells were re-suspended in growth media (α-Minimum Essential Medium-Alpha Eagle with 10% fetal bovine serum) and then plated for culturing. Cells were subcultured for up to six passages. CRISPR-Cas9 mediated KO cells were generated at passage 1 or 2. Cells from

individual subjects were used without pooling. Experiments were repeated in cells derived from at least three independent donors.

Generation of T-brites. Preadipocytes were plated in 12-well plates (5,000–15,000 cells/cm^2) were cultured to confluency. Two day-post confluent cells were induced to differentiate in complete differentiation media (Dulbecco's Modification of Eagle's Medium/F12 with 500 μM IBMX, 100 nM insulin, 100 nM dexamethasone, 2 nM T3, 101 g/ml transferrin, 1 μM rosiglitazone, 33 μM biotin, and 17 μM pantothenic acid) for 7 d followed by maintenance in Dulbecco's Modification of Eagle's Medium F12 supplemented with 33 μM biotin, 17 uM pantothenic acid, 10 nM insulin, and 10 nM dexamethasone for 3 d. After complete maturation into white adipocytes, the cells were treated with 1 μM Rosi for 7 d to generate T-brites. Additionally, to induce britening mature white adipocytes were treated for 7 d with 1 nM CL316,243 (β3 agonist), 100 nM FGF21, or 100 nM ANP.

DNA template engineering for in vitro transcription (IVT). We generated Cas9 nickase by site directed mutagenesis of humanized WT spCas9. The resulting vectors were utilized to PCR amplify the Cas9D10A and Cas9H840A fragments. An all-in-one nickase multi-cistronic mRNA template containing a 2A-linked puromycin cassette, which expresses Cas9 nickase and puromycin from a single ORF, was generated; the 2A peptide sequence was sandwiched between the Cas9 nickase and puromycin frames (Fig. 1d). The puromycin cassette was amplified from pCW-Cas9 (Addgene #50665). The 2A peptide [(GSG) A T N F S L L K Q A G D V E E N P G P], 5'UTR, and 3'UTR of human beta-globin were synthesized as gBlocks. To append a T7 promoter in front of the 5'UTR, we PCR amplified the 5'UTR gBlock with a primer containing a T7 promoter. Next, to generate all-in-one Cas9 nickase, we assembled all the inserts in a single reaction with Gibson assembly master mix (E2611, New England BioLabs Inc.). Following

Gibson assembly, purified all-in-one Cas9 nickase product was PCR amplified with All-in-One F1 (forward primer containing T7 promoter) and All-in-One R1 (reverse primer containing 10-nt oligonucleotide dT tail with 10T to assist poly A tailing). All intermediate PCR and Gibson assembly products were purified with QIAquick spin columns (Qiagen, Valencia, CA). The oligonucleotide sequences used in template construction are shown in Supplementary Table 1. All oligonucleotides were synthesized by Integrated DNA Technologies (Coralville, IA)

To generate mod mRNA templates for *CIDEA*, *LXRα*, *LXRβ*, *RXRα* and *GAPDH*, the ORFs of these genes were human codon optimized (https://www.idtdna.com/CodonOpt) and synthesized as gBlocks. The ORFs were identical to the NCBI human transcript variants (CIDEA: NM_001279.3, LXRα (NR1H3): NM_005693.3, LXRβ(NR1H2): NM_007121.5, RXRα (RXRA): NM_002957.5. In preliminary studies, 5'UTRs of AP2, beta-globin, CIDEA, and COL18A1 were appended to the GFP ORF along with the beta-globin 3'UTR. After examining the translation powers of GFP with different 5'UTRs through confocal microscopy, we chose the AP2 5'UTR for its high translational capacity in adipocytes. All UTRs were synthesized as gBlocks as described above.

To generate a 3× HA or 6×His tagged (N-terminus) *CIDEA* templates, AP2 5'UTR containing either tag sequence were synthesized as gBlocks. The AP2 5'UTR-3×HA or AP2 5'UTR-6×His were appended to the 5' end of the *CIDEA* ORF; the 3'UTR of beta-globin was appended simultaneously. The T7 promoter was appended in front of the 5'UTR. All sequences were assembled by Gibson assembly, as described above, and the purified products were PCR amplified with All-in-One F1 and All-in-One R1 primers (introduced above). Two NLS mutant CIDEA-HA constructs ($CIDEA_{K23A}$ –HA and $CIDEA_{R44A}$-HA) were generated from a *CIDEA*

ORF by nested PCR with mutant primers. The mRNA templates for these two mutants were constructed as described above.

Synthesis and purification of mod mRNA. Purified construct templates (0.1–4 μg) were produced by IVT with a MEGAscriptT7 kit (Ambion, Austin, TX, USA) in 50-μl IVT reaction mixtures containing, at a molar ratio of 1:1:1:0.2:0.7, the following constituents: (1) 7.5 mM ATP; (2) 7.5 mM 5-methylcytidine-5'triphosphate; (3) 7.5 mM pseudouridine triphosphate/2-thiouridine-5'-triphosphate; (4) 1.5 mM GTP; and (5) 5 mM for the cap analog (#1–4 from TriLink BioTechnologies, San Diego, CA; #5 from New England Biolabs, Ipswitch, MA). After IVT, mRNAs were polyadenylated (150~200 residues) using a poly(A) kit (Ambion). The IVT products were treated with Antarctic phosphatase (New England Biolabs) and the capped mRNAs that remained were purified with a MEGAclear kit (Ambion). The size and integrity of the mRNA products were verified by denaturing agarose gel electrophoresis.

Mod mRNA transfection. IVT mRNA was complexed to TransIT-mRNA (Mirus Bio, Madison, WI) according to the manufacturer's instructions in a reaction mixture containing 200 ng mRNA, 0.2 μl TransIT-mRNA reagent, and 0.15 μl Boost reagent in a final volume of 25 μl Opti-MEM (Invitrogen) medium (reagent quantities increased proportionately as needed). The mixture was incubated for 30 min before cell transfection.

Generation of hUCP1 Promoter-Enhancer reporter constructs and luciferase assay. To clone the human *UCP1* promoter-enhancer region, we designed *UCP1* promoter-enhancer-specific primers to amplify a 6.0-kb genomic region upstream of the human *UCP1* transcription start site (-6000 bp). The PCR product (6000 bp) was isolated from an agarose gel with a gel extraction kit (Qiagen) and cloned into a pGL3-basic vector. Several deletion constructs were

generated from PCR amplification (-4000 +1, -2800 +1, -1800 +1, -4000 -2800, -3800 -2800, -4000 -3850; primers in Supplementary Table 1) and cloned into the pGL3-basic vector. The Δ150bp deletion clone was generated by Gibson assembly of two overlapping PCR fragments [-6000 -4000 (2 kb) and -3850 +1 (3.850 kb)] and then cloned into a pGL3 basic vector. Multiple constructs containing DR1 and/or DR4 loss- and gain-of-function mutants (DR1-ΔDR4 = 134 bp, DR4-ΔDR1 = 137 bp, DR4 - 3XDR1 = 178bp, and 3XDR4-DR1 = 184 bp) were designed and synthesized as gBlock gene fragments (Invitrogen) and then cloned into pGL3-LUC vectors. pGL3-LUC vectors were then reverse transfected into differentiated human brite adipocytes with 2 µl/µg DNA of lipofectamine 2000 (Invitrogen) according to the manufacturer's instructions, and then 48 h later, the cells were transfected with mod mRNAs [*GAPDH* (control), *CIDEA*, *LXRα*, *LXRβ*, and *RXRα*]. After 24 h of mod mRNA treatment, cells were treated with isoproterenol, Rosi, and T09 (only when LXRα/β was exogenously expressed) in the adipocyte maintenance media. The cells were harvested 12 h later and their luciferase activities were measured with a Promega Dual-Glo Luciferase Assay System. Values were normalized relative to the Renilla signal to allow for differences in transfection efficiency.

***In vitro* DNA pull-down assay in a cell-free system.** DNA pull-down assays were performed based on a previously described protocol (Deng et al. (2003) Anal Biochem *323*, 12-18). Briefly, the 150-bp distal hUCP1 promoter region was amplified from human genomic DNA by PCR (Applied Biosystems) with biotinylated primers (Integrated DNA technologies; Supplementary Table 1) and platinum Green Master Mix (Invitrogen) under the following conditions: 94 °C for 5 min, forty 45-s 94-°C cycles, 58 °C for 30 s, 72 °C for 90 s, and 72 °C for 10 min. Additionally, 20-mer biotinylated and non-biotinylated (competing) DR1 and DR4 oligonucleotides corresponding to the 150-bp distal hUCP1 enhancer were synthesized

(Integrated DNA Technologies). *In vitro* translated proteins (hCIDEA, hLXRα, hRXRα, and hPPARγ; 10 μg each) were preconditioned with streptavidin magnetic beads (Dynabeads M270, Thermo-Fisher) for 30 min at 4 °C, and then incubated with 2 μg biotinylated double-stranded DNA or 500 pmol biotinylated/non-biotinylated oligonucleotides overnight at 4 °C in a rotating shaker. The next day, DNA-protein-streptavidin-magnetic bead complexes were pulled down by magnetic stands for 5 min. The supernatants was discarded and the complexes were washed twice with cold Tris buffered saline (TBS). The beads were re-suspended in 25 μl of 2× sodium dodecyl sulfate (SDS) buffer, boiled at 95 °C for 5 min, and then the proteins were separated by SDS-polyacrylamide gel electrophoresis (PAGE) followed by western blotting with indicated antibodies. Non-biotinylated (competing) oligonucleotides were used as a control as well as to compare the strength of their biotinylated counterparts.

For *in vitro* crosslinking of the CIDEA-LXRα complex with DR4 followed by streptavidin-biotin pull down, short-arm (HCHO) and long-arm (EGS) crosslinkers were utilized (Zeng et al. (2006) Biotechniques *41*, 694, 696, 698). The DNA-protein-streptavidin magnetic bead complexes were incubated with either 1% HCHO for 15 min alone or in 1.5 mM EGS for 30 min and then in 1% HCHO for 15 min. The crosslinking reaction was stopped with 50 mM glycine-PBS for 10 min, and the crosslinked mixture was centrifuged at 300 ×*g* for 2 min followed by washing, as described above.

***In vitro* DNA pull-down assay.** Adipocyte nuclear extraction was performed with NE-PER™ nuclear and cytoplasmic extraction reagents (Thermo-Fisher) according to the manufacturer's protocol. Following nuclear extraction, 500 μg of lysate was incubated with 5 μg biotinylated DNA probes and 200 μl streptavidin magnetic beads. The final volume was adjusted to 500 μl with NER buffer from the kit. The mixture was placed on a rotating shaker and incubated

overnight at 4 °C. The samples were placed on a magnetic stand, washed with ice cold PBS three times, and washed once with NER buffer.

ChIP assays. ChIP assays were performed with a ChIP-IT assay kit (Active Motif, Carlsbad, CA) according to the manufacturer's instructions. Briefly, 1% HCHO-fixed chromatin was isolated from T-brites following glycine quenching. After sonication shearing of chromatin, crosslinked protein-DNA complexes were pre-cleared with protein-G-agarose and incubated with protein G-coated magnetic beads bound with LXRα. Complexes were precipitated with magnetic beads and the DNA was released, purified, treated with protease, and finally analyzed by real-time PCR with appropriate primers (Supplementary Table 1). Controls included anti-RNApol II (positive), mouse IgG (negative), and non-reactive anti-GAPDH (negative) for immunoprecipitations and a set of random oligonucleotides for control PCR.

IVTT and DNA template construction. IVTT constructs were generated following the guidelines of Pierce's PCR protocol for generating optimized templates (TR0072.1). A 600-bp T7-IRES-Kozak sequence containing a T7 promoter, internal ribosome entry site, and Kozak sequence were amplified from pT7CFE1 vectors (no. 88860) with T7 sense and Kozak anti-sense primers. Next, an overlap sense primer (overlap with Kozak sequence) and an overlap anti-sense primer (overlap with gene ORF or fragments) containing a 30-nt poly-A sequence were utilized to amplify the gene ORF (*CIDEA*, *LXRα*, *RXRα*, or *PPARγ*) or gene fragment ($CIDEA_{1\text{-}70aa}$, $CIDEA_{33\text{-}110}$, $CIDEA_{1\text{-}160aa}$, $CIDEA_{71\text{-}160aa}$, $CIDEA_{160\text{-}219aa}$, $CIDEA_{70\text{-}184aa}$, $CIDEA_{184\text{-}219aa}$, $CIDEA_{1\text{-}219\Delta\Delta aa}$, $LXR\alpha_{1\text{-}96aa}$, $LXR\alpha_{97\text{-}200aa}$, $LXR\alpha_{205\text{-}447aa}$, or $LXR\alpha_{215\text{-}434aa}$). These two fragments were combined for overlap extension PCR with T7 sense and overlap anti-sense primers. PCR cycles were performed according to the guidelines. The resulting PCR templates were purified, and the identities of the templates were confirmed by restriction enzyme analysis; 1 μg of template DNA

was utilized for 50 µl of transcription-translation reaction mixture with a 1-Step Human Coupled IVT Kit according to manufacturer's recommendations (Thermo-Scientific). A sample without added DNA was used as a negative control; GFP template DNA was used as a positive control. Translation reaction time was optimized for protein length to reduce truncated proteins due to material exhaustion. The reaction times were as follows: 1–100 aa = 360 min, 101–200 aa = 240 min, 201–300 aa = 180 min, 301–500 aa = 120 min, >501 aa = 90 min. Following translation, total protein concentration was calculated and small portions were subjected to western blotting to confirm protein integrity or placed in -80 °C storage for co-IP.

***In vitro* CRISPR-Cas9D10A DNA cleavage assay in a cell-free system.** To test the *in vitro* efficacy of the CRISPR/hCas9D10A system, we used IVTT synthesized hCas9D10A protein. This Cas9 protein (1 µg) was incubated with each gRNA (50 nM) and the PCR amplified human CIDEA sequence (500 ng) containing all exons. This reaction was performed in 1×NEB buffer 3 with 1×NEB BSA at 37 °C for 1 h. Following treatment with RNase (Invitrogen) and 0.5 µl proteinase K (molecular biology grade, New England Biolabs) for 15 min at 37 °C, *CIDEA* DNA fragments resulting from CRISPR/hCas9D10A-induced cleavage were analyzed by agarose gel electrophoresis.

T7E1 assay. We extracted genomic DNA from cells 3 d after nucleofection using a DNA isolation kit for cells and tissues (Sigma-Aldrich) following the manufacturer's instructions. PCR amplicons spanning the sgRNA genomic target sites (*CIDEA* exon 4) were generated with Platinum Hot Start PCR Master Mix (2×)(Thermo-Fisher) with the indicated primer pairs. PCR amplicons were purified, from which 250 ng was denatured, re-annealed in a thermocycler, and digested with T7EI (New England Biolabs, Waltham, MA) in accordance with the manufacturer's protocol. Digested DNA was run on a 5% TBE polyacrylamide gels, stained with

ethidium bromide solution (Sigma-Aldrich), and visualized on a ChemiDoc (Bio-Rad). Band intensities were analyzed with Image Lab Software (Bio-Rad) and allele modification frequencies were calculated as follows: $100 \times [1 - (1 - \text{fraction cleaved})^{0.5}]$.

CRISPR/Cas9 Nickase mutagenesis. Freshly isolated hADsc were plated in 10cm dish. At passage 1 the confluent cells (~80%) were forward and reverse transfected with 5-30 µg of hspCas-D10A mod RNA. After 12 hrs of transfection, puromycin (1.5 µg/ml) was added in the culture media to create a positive selection pressure. Additionally, after 48hrs of Cas9 nickase mod mRNA transfection, modified sgRNA pair (1 & 2) was reverse transfected. The transfection mixture also contained AZT (5 µM concentration) (Azidothymidine, sigma) a small molecular CRISPR indel enhancer. After another 72hrs of puromycin selection (0.5 µg/ml), the remaining cells were trypsinized and re-plated in 12 wells plates at a seeding density of 1×104 cells/well with equivalent mixture of pre-adipocyte GM and pre-adipocyte conditioned media. This media was supplemented with rho associated protein kinase inhibitor Y-27632 to increase the clonal population. After 5 days of expansion, cells were harvested to isolate genomic DNA for T7 E1 assay. CIDEA transcript and protein was completely absent in preadipocytes. Therefore, to check the loss of function of CIDEA, we induced CIDEA transcription in these nonconfluent preadipocytes by 12 hr incubation in adipocyte differentiation media, containing 0.1 µM Rosi. To measure the loss of function, we designed five sets of real time primers targeting each exon or exon intron boundary. Of two primers targeting CIDEA exon 4, one primer was designed to locate between two sgRNA. It is expected that Cas9 Nickase mediate indel would not interfere with another exons transcription.

***In situ* protein-protein interaction PLA.** The mouse/rabbit red starter Duolink kit (DUO92101, Sigma-Aldrich) was used according to the manufacturer's protocol. Briefly, Rosi-induced,

terminally-differentiated human WT (CIDEA$^{+/+}$) or KO (CIDEA$^{-/-}$) T-brites were cultured on lysine-coated coverslips (Sigma-Aldrich), fixed with 4% paraformaldehyde for 15 min, and quenched with 2% glycine for 15 min. Next, cells were permeabilized with 0.025% Triton-x in TBS with 0.1% Tween 20 (TBST), blocked for 1 h, and then incubated with the indicated primary antibodies overnight in TBST. Cells incubated with primary antibodies only or with/without PLA probes only (mouse and rabbit) were assay controls. The cells were then incubated with oligonucleotide-conjugated PLA probes for 60 min followed by ligation of PLA probes in a preheated humidified chamber for 30 min at 37 °C. The signal was amplified for 100 min in same humidified chamber and visualized under a Nikon confocal microscope.

Immunofluorescence and western blotting. Confocal microscopy was performed with a Zeiss LSM 710-Live Duo scan (Carl Zeiss, Oberkochen, Germany) or Nikon A1R (Nikon, Japan) with a 60× or 100× oil immersion objective. For immunofluorescence, hADSCs that had been differentiated into T-brites on poly-L-lysine coated glass cover slips in 24-well plates and transfected (24 h before sample preparation) with TransIT-mRNA (Mirus Bio, Madison, WI) were fixed with 4% para-formaldehyde (10 min), and then placed, in series, in 2% glycine (10 min), 0.025% Triton X-100 (5 min), PBST (3 times for washing), 10% goat serum B (10 min), and primary antibodies in TBST with 4% goat serum (overnight, 4 °C). Coverslips were washed three times with PBST and incubated for 2 h in the dark with secondary antibodies (Alexa Fluor 488 or 594, in PBST with 4% goat serum). Cells on coverslips were washed three times with PBST before LD staining with HCS LipidTOX-Deep Red or HCS LipidTOX Red (Invitrogen) for 20 min. Finally, the cells were washed with PBS three times before mounting on glass slides with Vecta Shield media (Vector Labs, CA) with or without 4',6-diamidine-2'-phenylindole

dihydrochloride nuclear counterstain. Images were processed with ImageJ and Adobe Photoshop®.

For western blotting, cells were lysed in 1× lysis buffer (Roche) supplemented with phosphatase and protease inhibitors (1 μg/ml aprotinin, 1 μg/ml pepstatin, 1 μg/ml leupeptin, 1 mM phenylmethane sulfonyl fluoride, and 1 μg/ml trypsin inhibitor) and 1% Triton X-100, followed by sonication and incubation on ice for 2 h. Subsequently, the cells were centrifuged at 7,500 rpm for 30 min at 4 °C. The supernatants were collected and protein quantities was estimated by the Bradford method; 25–50-μg total protein aliquots from each sample were resolved by 10–12% SDS-PAGE.

Mitochondrial DNA copy number and total oxidative phosphorylation protein analysis. To quantify mitochondrial DNA in WT and KO T-brites, total cellular mitochondria were isolated with an Abcam mitochondrial isolation kit (ab110171) according to the manufacturer's instructions. Mitochondrial DNA copy number was quantified with primers specific for the mitochondrial D-loop region and nuclear genome specific β2 microglobulin by quantitative PCR. The mtDNA copy number/cell is represented by the D-loop:nuclear target ratio.

For oxidative phosphorylation protein analysis, 20 μg of mitochondria was denatured in SDS sample buffer for 5 min at 50 °C and then separated in 4–12% Bis/Tris gels (3-morpholinopropane-1-sulfonic acid buffer). Transfer membranes were blocked in 4% BSA-TBST for 4 h at room temperature, and then incubated with a primary antibody cocktail (1:1000; Abcam, ab110411) for 4 h at room temperature. After three washes with TBST, the membranes were incubated with horseradish peroxidase-conjugated goat-anti-mouse secondary antibody

(1:10000) for 1 h at room temperature. Peroxide activity was visualized by enhanced chemiluminiscence and exposure to x-ray film.

UCP1 promoter- enhancer analysis and CIDEA NLS prediction. The human UCP1 promoter- enhancer sequence was downloaded from the UCSE browser and confirmed to be a strong match for the human sequence in ENSEMBL. A transcription start site was annotated in a CpG island-rich region. Multiple putative LXREs were identified in the vicinity of a primate-specific Alu element in both strands. Binding efficiencies were calculated based on the most conserved consensus DR4-LXRE motif (ACGTCA-TAAA-GGGTCA). A binding strength ≥ 0.5 was considered strong. We aligned orthologous human and mouse *UCP1* promoter sequences in CLUSTALW and determined the maximum conservation score around LXRE/RXR. We utilized several programs to analyze the promoters: http://cisreg.cmmt.ubc.ca/cgi-bin/tfe/home.pl; http://www.cisreg.ca/cgi bin/mscan/MSCAN; github.com/amathelier/DNAshapedTFBS; http://alggen.lsi.upc.es/cgi-bin/promo_v3/promo/promoinit.cgi?dirDB=TF_8.3; and http://opossum.cisreg.ca/oPOSSUM3/. We used SeqNLS (lin and Hu (2013) PLoS One *8*, e76864), cNLS Mapper (lin and Hu (2013) PLoS One *8*, e76864), and NucPred (Brameier et al. (2007) Bioinformatics 23, 1159-1160) for NLS prediction of the human CIDEA protein sequence (NP_001270.1).

Cycloheximide and FFA mixture chase assay. Following a 6-h incubation in ISO, mature T-brites were subjected to chase assays with 30 μg/mL CHX or 5% FFAs and then harvested immediately or 3 h, 6 h, 18 h after treatment. Nucleus/LD fractions isolated by subcellular fractionation (described above) were subjected to western blotting with indicated antibodies.

Quantification of gene expression by real time PCR. Total RNA was isolated from differentiated adipocytes with TRIzol and cDNAs were synthesized with a M-MuLV reverse transcriptase kit (MBI Fermentas, USA). Real-time PCR was performed with Power SYBR green dye in a Step One Plus Real Time PCR System (Applied Biosystems, Foster City, CA) according to the following program: 95 °C for 10 min, 35 15-s cycles at 95°C, 55–61°C for 30 s, 72 °C for 30 s, and a final melting curve step. The collected CT values were normalized to an internal control, peptidylprolyl isomerase. There were five determinations using five individual experiments. The results (mean ± standard errors) were expressed as fold changes relative to the same gene in control human differentiated adipocytes.

Seahorse bioenergetic analysis. Approximately 15,000 hADSCs at passage 4 were seeded in 100 µl media/well of an XF24 V7 plate for OCR measurement at 37 °C by an XF24 analyzer (Seahorse Bioscience). On day 8 of differentiation, 2 h before OCR measurement, human britening media was replaced with pre-warmed Seahorse XF assay medium (supplemented with 20 mM glucose, 1 mM Na-pyruvate, 2 mM GlutaMax, 0.8 mM Mg^{2+}, 1.8 mM Ca^{2+}, 143 mM NaCl, 5.4 mM KCl, 0.91 mM NaH_2PO_4, and 15 mg/l phenol red, pH 7.4) and incubated at 37 °C in an air incubator (without CO_2) for 45–60 min. Mitochondrial assay compounds were loaded into injection ports (50 µl/port) and four assay cycles (cycle: 1 min mix, 3 min wait, 3 min measuring period) were used to determine basal respiration, and then ATP coupled respiration was inhibited by 5 µM oligomycin. Maximum respiratory capacity was assessed after addition of 1 mM FCCP (Tocris). Finally, mitochondrial respiration was blocked by injection of a 1:1 mixture of rotenone and antimycin A (5 µm each; Tocris) to correct for non-mitochondrial respiration rate. FCCP was injected with Na-pyruvate (10 mM); other compounds were injected with assay medium. ISO (1 µM) was injected to measure the contribution of UCP1 mediated

uncoupled respiration. For some experiments, cells were pretreated with orlistat (50 μM) or CSA (5 μg/ml) for 1 h in human britening media. Both were present at same concentration in the assay medium during ISO mediated stimulation. In a separate experiment, TTNPB (0 μM, 5 μM, 10 μM, 25 μM, 50 μM, and 100 μM in DMSO) or nonanoic acid (0 μM, 5 μM, 10 μM, 25 μM, 50 μM, and 100 μM) was injected with assay medium to determine the effective TTNPB concentration. OCRs were calculated in Seahorse XF-96 software. Data were exported and reconstructed in GraphPad Prism 5.0 software. After completion of each assay, proteins were isolated from each well for UCP1 expression FABP4 expression determination. Each experiment was repeated 3–5 times with similar results.

Cellular import assay. *In vitro* nuclear transport assays were conducted as previously described (Wagstaff et al. (2012) Biochem J *443*, 851-856; Whitehurst et al. (2002) Proc Natl Acad Sci U S A *99*, 7496-7501) with minor modifications. For analysis of the influence of Impα/β on CIDEA import, we treated T-brites with 5 μM of ivermectin (Sigma) at the same time as CIDEA-HA and SV40-T-Ag-HA mRNA transfection. Cells were fixed and subjected to immunofluorescence 24 h later. To check whether CIDEA import depends on active transport, T-brites on coverslips were washed with import buffer (20 mM HEPES, 110 mM potassium acetate, 2 mM magnesium acetate, 1 mM EGTA, and 2 mM dithiothreitol). To deplete cellular internal transport factors, cells were permeabilized with digitonin (50 μg/ml; Sigma) in import buffer for 5 min on ice. For the energy-dependence experiments, an energy regenerating transport mixture (50 μl/coverslip) was prepared by mixing 25 μl rabbit reticulocyte lysate (Promega) with 25 μl import buffer containing 1 mM ATP, 0.1 mM GTP, 5 mM creatine phosphate, and a protease inhibitor mix (source or recipe). To measure the energy-dependent import of substrates (CIDEA and SV40-T-Ag), CIDEA-HA, and T-Ag-HA were translated *in vitro* as described above. The substrates were

added to a final concentration of 5 μg/50 μl in the transport mixture and then 50 μl of the transport mixture was added drop-wise to cover each whole coverslip, and the mixture was incubated in a cell culture incubator for 60 min. The cells were washed, fixed with 4% paraformaldehyde, and subjected to immunofluorescence with anti-HA primary antibody. To generate an energy depleted import mixture, rabbit reticulocyte lysates were pretreated with apyrase (25 U/ml, New England Biolabs) at 30 °C for 30 min before adding the import mixture (also ATP-, GTP-, and creatine phosphate-free) to the cells.

Quantification of protein-DNA interaction strength with the modified restriction fragment length polymorphism (RFLP) method. We used the $dUER_{150bp}$ (i.e., 150-bp UCP1 distal enhancer region containing DR1 and DR4) sequence as target DNA, with a unique AatII restriction site (GACGT*C/C*TGCAG) created by site directed mutagenesis (T>A) near the DR4 sequence by nested PCR with mutant primers (Supplementary Table 1). Target DNA (500 ng) was incubated at 37 °C for 30 min in reaction buffer (1× NEB 1× CutSmart® buffer) with *in vitro* translated LXRα and RXRα (5 μg each) in a final volume of 50 μl. Following incubation with LXRα, *in vitro* translated CIDEA or BSA (1–5 μg) was added to the reaction mixture, which was then incubated at 37 °C for an additional 30 min. The post-CIDEA reaction mixture was incubated with 5 U of AatII restriction enzyme at 37 °C for 45 min. The digested DNA was resolved in a 2.5% agarose gel and visualized by DNA staining. Cleavage efficiency was determined as the intensity ratio of cleaved to uncleaved bands in ImageJ. The ΔDR4 150-bp target cleavage and 150-bp target cleavage in the presence of BSA were utilized as controls. The strength of AatII-mediated LXRα bound DR4 cleavage is directly proportional to the amount of CIDEA in the reaction.